PNNL-36532
M3LW-24OR0404013

Light Water Reactor Sustainability Program

Thermal aging effects on crosslinked polyethylene cable insulation with decabromodiphenyl ether flame retardant alternative

Yelin Ni, Md Kamrul Hasan, Tyler R. Tueller, Kumari Sushmita, Mychal P. Spencer, Andrew G. Smith, Muthu Elen, Vishal Kumar, Leonard S. Fifield

Pacific Northwest National Laboratory

September 2024

U.S. Department of Energy

Office of Nuclear Energy

PNNL-36532
M3LW-24OR0404013

Thermal aging effects on crosslinked polyethylene cable insulation with decabromodiphenyl ether flame retardant alternative

Yelin Ni, Md Kamrul Hasan, Tyler R. Tueller, Kumari Sushmita, Mychal P. Spencer, Andrew G. Smith, Muthu Elen, Vishal Kumar, Leonard S. Fifield

Pacific Northwest National Laboratory

September 2024

Prepared by
Pacific Northwest National Laboratory
Richland, WA 99354
operated by
Battelle
for the
U.S. Department of Energy
under Contract DE-AC05-76RL01830

CONTENTS

LIST OF FIGURES

LIST OF TABLES

EXECUTIVE SUMMARY

Decabromodiphenyl ether (decaBDE) has been extensively used as a flame retardant in several applications, including nuclear electrical cable insulation. However, decaBDE has been identified as a persistent, bioaccumulative and toxic (PBT) substance, leading to regulatory scrutiny. The Environmental Protection Agency (EPA) published a regulation on January 6, 2021, aimed at phasing out the manufacturing, processing, and distribution of decaBDE. This rule set a compliance deadline of March 8, 2021, for the manufacture and processing of decaBDE, and an extended deadline of January 6, 2023, for specific applications including wire and cable insulation in nuclear power generation facilities.

In response to such regulations, RSCC, a major supplier of safety-related electrical cables and associated products to the U.S. nuclear industry updated the formula of their crosslinked polyethylene (XLPE) insulation to replace the historically used decaBDE flame retardant with an acceptable alternative. This change from the previous decaBDE-containing XLPE prompted interest in comparative performance of the two material formulations, especially with respect to characteristics relevant to safety-related function such as thermal and radiation resistance. RSCC graciously provided samples of wire insulated with the decaBDE-containing XLPE formulation and corresponding wire insulated with XLPE of the new formulation, containing a decaBDE alternative. In this work we compare characteristics of the two formulations and a previously produced commercial version of the RSCC decaBDE-containing XLPE insulation subjected to thermal aging at 150 °C and 165 °C. The comparison was focused on mechanical durability, thermal stability in the oxidative environment, and chemical structures.

Briefly,

- Tensile elongation at break (EAB) results showed loss of mechanical elasticity with longer aging time, as expected. Aging time dependence of EAB did not differ between the decaBDE-containing and decaBDE-alternative samples.
- Subtle differences between the two materials can be detected from Fourier-transform infrared spectroscopy (FTIR) absorbance spectra in the range below 1700 cm^{-1}, are assumed to be related to decomposition of flame retardant additives during thermal aging.
- The oxidation induction time (OIT) data seemed to show that the unaged decaBDE-containing XLPE material is more thermally stable than the unaged decaBDE-alternative material, but the discrepancy in OIT decreased with aging time and the OIT values of the two materials became similar starting with the 4^{th} day of aging at 165 °C.

This thermal aging investigation confirmed that the mechanical durability, a key property monitored for cable qualification, was not significantly affected by the modification of the formulation with a decaBDE alternative flame-retardant system in the investigated thermal aging conditions. Further studies on the same sets of materials exposed to thermal and gamma radiation aging would further inform comparison of the materials safety-related function.

ACKNOWLEDGEMENTS

This work was sponsored by the U.S. Department of Energy, Office of Nuclear Energy, for the Light Water Reactor Sustainability (LWRS) Program Materials Research Pathway. The crosslinked polyethylene electrical cable materials studied herein were graciously provided by RSCC through Eric Rasmussen and Jeffrey Schroeder. The authors extend their appreciation to Pathway Lead Dr. Xiang (Frank) Chen for LWRS programmatic support. This work was performed at the Pacific Northwest National Laboratory (PNNL). PNNL is operated by Battelle for the U.S. Department of Energy under contract DE-AC05-76RL01830.

1. INTRODUCTION

Organic electric cable insulation polymers are primarily composed of carbon and hydrogen and are inherently combustible. A combustion reaction involves combustibles (e.g., polymers), combustive (e.g., oxygen), and heat (Laoutid 2009). The volatile fractions produced during chain scission of polymers diffuse into the air and create a combustible gaseous mixture (fuel), which could ignite when an auto-ignition temperature is reached (Laoutid 2009). The ignition could proceed at a lower temperature (flash point) upon reaction with an external source of intense energy (e.g., spark, flame) (Laoutid 2009) .

Flame retardant systems are intended to inhibit or stop the polymer combustion process either physically (by absorbing heat, forming a thermal shielding char layer, diluting the flammable gases) or chemically (Laoutid 2009). Flame retardancy through chemical modification can be achieved by converting the highly reactive free radicals ($H\cdot$ and $OH\cdot$) in the gaseous or the condensed phase into less reactive or inert molecules, typically using flame retardant additives that can release $Cl\cdot$ and $Br\cdot$ radicals (Laoutid 2009). In addition to scavenging existing flammable species, the reaction is also endothermic and can reduce temperature thereby reducing further production of gaseous fuels (Laoutid 2009).

Crosslinked polyethylene (XLPE) and ethylene propylene rubber (EPR) represent the most used base polymer types in nuclear grade electrical cable insulation (Fifield et al. 2023). XLPE and EPR insulations require flame retardant additives, as opposed to chlorinated polyethylene or chlorosulfonated polyethylene that are intrinsically flame retardant (EPRI 2017). Below are the major categories of flame-retardant additives for low voltage power cables:

- Hydrated minerals, e.g., $Mg(OH)_2$ and $Al(OH)_3$, which physically cool down fuel through the endothermic hydrolysis reaction and dilute the fuel with a non-flammable gas;
- Brominated compounds, including brominated ethers, brominated diphenyl compounds, and brominated cyclohydrocarbons, which release $Br\cdot$ radicals that react with fuel radicals;
- Chlorinated compounds, e.g., chlorinated paraffin waxes, which are also a reactive type of flame retardant;
- Phosphate compounds, e.g., triaryl phosphates, resorcinol diphenyl phosphate (RDP), phosphinic acid compounds, and ammonium polyphosphate (APP), which promote char formation and inhibit flame propagation in the gas phase.

Certain brominated compounds have come under significant regulatory attention for their potential as persistent, bioaccumulative and toxic (PBT) chemicals, including decabromodiphenyl ether (decaBDE, Figure 1) and octabromodiphenyl ether (octaBDE) (EPRI 2017). OctaBDE is no longer manufactured due to regulations that have been imposed in most countries, with some exceptions (EPRI 2017). DecaBDE is faced with prohibition by the Environmental Protection Agency (EPA). On January of 2021, EPA published the final rule, 86 FR 880, aiming at phasing out the manufacturing, processing, and distribution of decaBDE or decaBDE-containing products (Federal Register 2021). This rule set a compliance deadline of March 8, 2021, for the manufacture and processing of decaBDE, and an extended deadline of January 6, 2023, for specific applications including wire and cable insulation in nuclear power generation facilities (Federal Register 2021).

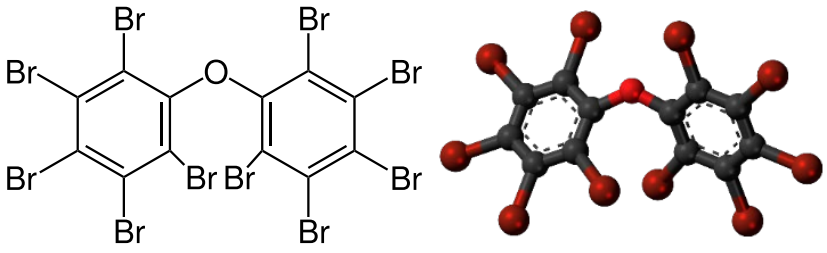

Figure 1. Chemical structure of decabromodiphenyl ether (decaBDE)

Since decaBDE has long been relied upon as the flame retardant in one of the most common XLPE nuclear cable insulation formulations, RSCC Firewall III insulation, questions have naturally arisen regarding whether changes in cable performance might be expected for XLPE containing a decaBDE alternative, especially for safety-related cables that must perform their safety function in a design basis event such as a loss of coolant accident. The research described here aims to directly investigate observable differences in material performance of the standard historical decaBDE-containing XLPE insulation and of the newly formulated XLPE, containing a decaBDE alternative, for samples subjected to accelerated thermal aging. Thermal oxidation, mechanical, and chemical properties of XLPE samples provided by the manufacturer with and without decaBDE were determined.

2. EXPERIMENTAL

2.1 Materials

Descriptions of the three types of polymer insulation used in this study are given in Table 1. The base polymer is crosslinked polyethylene (XLPE). Spools of XLPE-D (containing decaBDE) and XLPE-N (with decaBDE alternative) cables were provided by RSCC for this project. The XLPE-C (commercial) was purchased in the past from RSCC and is understood to have a similar decaBDE-containing formulation to XLPE-D.

Figure 2. DecaBDE containing XLPE cable insulation on a spool.

Table 1. Information of cable insulations investigated.

Material ID	Prints on insulation or jacket	Color	Release date
XLPE-D (with decaBDE)	1/C 14 AWG COPPER RSCC XLPE KXL-760G DECABDE ZZU2301-001 2024	White	2023
XLPE-N (with decaBDE alternative)	1/C 14 AWG COPPER RSCC XLPE KXL-760G NON-DECABDE ZZU2301-002 2024	White	2023
XLPE-C (commercial)	2/C 16 AWG COPPER RSCC 600V FIREWALL III FRXLPE SHIELDED CSPE	Grey	2015

2.2 Sample Preparation

Insulated wires were sectioned into 120 mm long samples and the metal conductors were removed prior to thermal aging. Figure 3(a) shows the layout of the insulation stripping tool and the cables to be cut. A cable stripper (The Eraser Company, Inc, Model LSR10) was clamped on the bench with two C-clamps. Die blades of 0.079" (part # IR1707) were used both for XLPE-D and XLPE-N insulations. The insulated wire from the spool was placed on the black movable platform, in between two rubber-covered clamps and through the hold of die blade halves. As shown in Figure 3(b), when the handle was pulled, the blade halves closed, the platform moved in the same direction as the handle (downward in Figure 3(b)), and the cable clamps rotated in the opposite direction to secure the insulation when the insulation was pulled away from the blades (downward in Figure 3(b)). The insulation from the spool was scored at the die blades, and the conductor wires were pulled from the scored location to leave the stripped insulation between the blade and the stopper, as shown in Figure 3(c). Final length of samples was determined by the length between stopper and blade, which was set to 120 mm in this study, as shown in Figure 3(d).

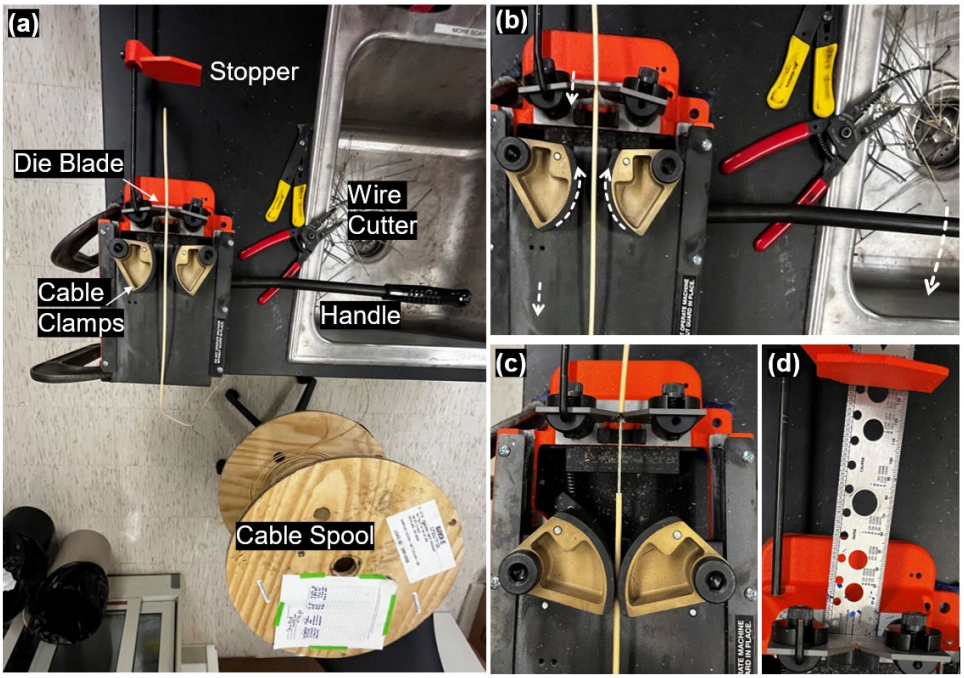

Figure 3. Stripping tools to remove metal conductor from cable insulation.

XLPE-C samples were stripped in the past using pliers to pull the outer layer of the insulation while securing the exposed metal conductors on a vise and were cut into 100 mm in length.

2.3 Aging Conditions

Figure 4(b) shows a photo of the aging ovens (Thermo Scientific, Heratherm OMH180) used in this study. Samples cut into 120 mm (XLPE-D and XLPE-N) or 100 mm (XLPE-C) were hung on a rack with alligator clips and paper clips on one end of each, as shown in Figure 4(c). The racks were placed inside the oven as shown in Figure 4(a).

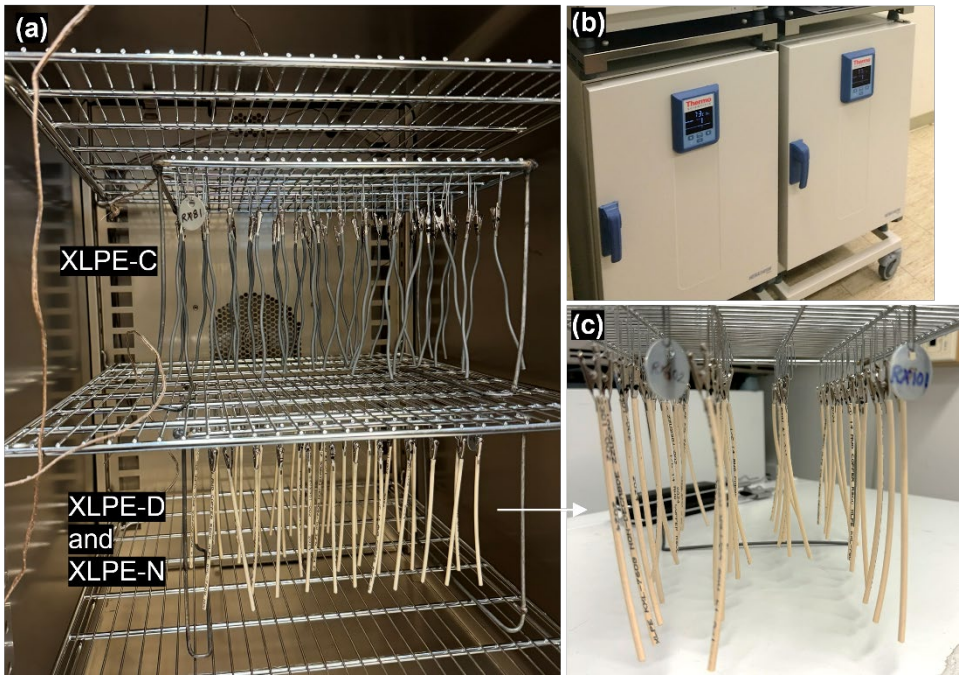

Figure 4. Insulation samples hung on a rack (a) inside and (c) outside the (b) aging ovens.

Temperatures measured by type-K thermocouples (Figure 4(a)) were recorded every 5 min by a datalogger (Omega RDXL6SD). Temperatures were set to 150 °C and 165 °C. The actual temperatures are plotted in Figure 5. Points of temperature drop were caused by opening of the oven to retrieve the samples aged on the target days. Aging at 150 °C started at day 0 in Figure 5, while the aging at 165 °C started from the second week. During the first week, the fan speed of the 165 °C oven was adjusted until the temperature reading of thermocouples was at 165 ± 0.5 °C. Aging at 165 °C was terminated after 10 days. A second period of aging at 165 °C started on the 55th day until significant loss of mechanical elasticity was detected for the aged samples, resulting in a total of 20 days of aging at 165 °C for samples used for mechanical testing.

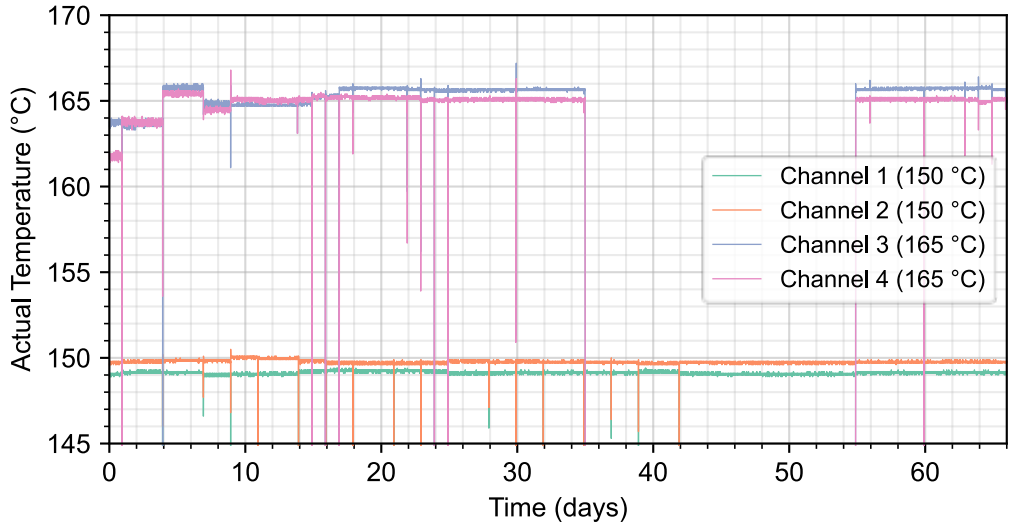

Figure 5. Temperature readings of 4 datalogger channels with thermocouples inserted into the ovens set to 150 °C and 165 °C.

2.4 Characterization

2.4.1 Tensile Elongation at Break (EAB)

Uniaxial tensile testing was performed following IEC/IEEE 62582-3, from which EAB was obtained. After aging, the samples were conditioned for 48 hours in an environmental chamber (Caron Model 7000-25) controlled at 23°C ± 2°C and 50% ± 10% relative humidity, per ASTM D618 Procedure A.

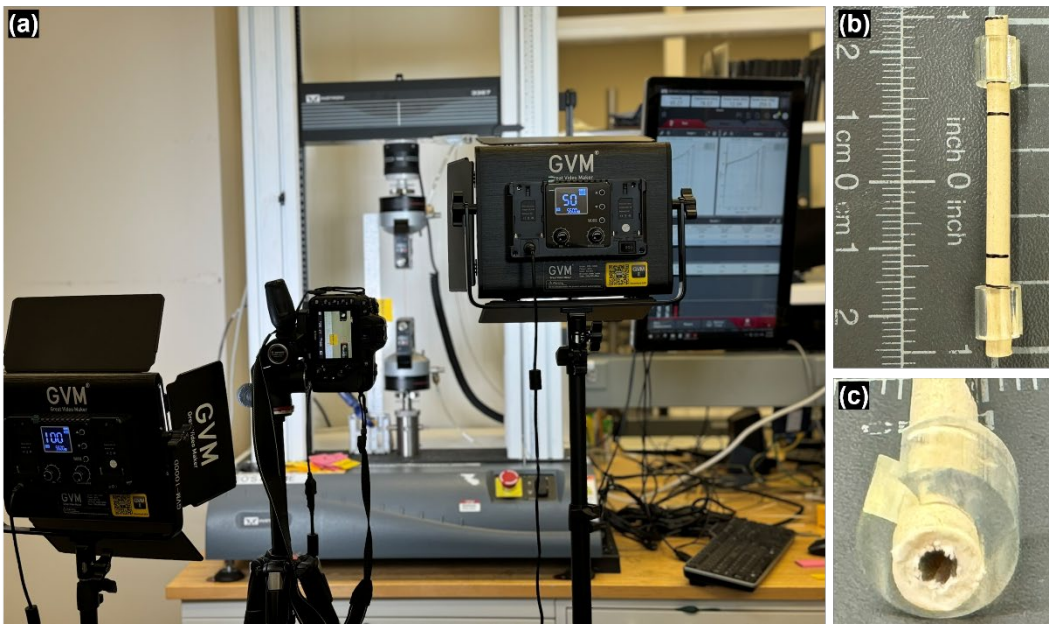

Figure 6. (a) Layout of the tensile testing setup. (b) Gauge marks on an XLPE-D sample. (c) End tab of an XLPE-D sample.

The sample was cut to 50 mm and tested on an Instron 3360 test frame equipped with a 1 kN load cell and pneumatic grips. The grip pressure was set to 15 ~ 20 psi. As shown in Figure 6(c), end tabs were used to prevent slippage or crushing of the sample by grip pressure. The end tab was cut from a polyurethane tube

into an approximately 8 mm length and was placed 1~2 mm from the ends of samples. As shown in Figure 6(a), videos of sample breaking were recorded by a digital camera for strain calculation with home-built extensometer software. Gauge marks were drawn on samples to assist strain detection, as shown in Figure 6(b) where two black gauge marks at 20 mm separation were drawn with an ultrafine permanent marker. The grip separation was 30 mm. A pull rate of 10 mm/min was used to minimize premature failures. Data points were removed if the samples did not break within the gauge section (such as at the grip).

2.4.2 Oxidation Induction Time (OIT)

OIT was measured following IEC 62582-4 on a differential scanning calorimeter (DSC Q2000, TA Instruments, see Figure 7) with the RSC90 cooling accessory. DSC was calibrated per ASTM D4565 using indium and tin standards. A Tzero pan was used to contain a thin slice of insulation sample of 5 ~ 10 mg. Pan lids were not used. Samples were heated in a N_2 atmosphere at 50 mL/min gas flow rate at a heating rate of 20 °C/min up to 220 °C. After equilibrating at 220 °C for 5 min, the cover gas was switched to pure O_2. The temperature was kept at 220 °C for a certain period, varying from 20 min to 2 h, until an exothermic peak was observed.

Figure 7. Differential scanning calorimeter for oxidation induction time (OIT) testing.

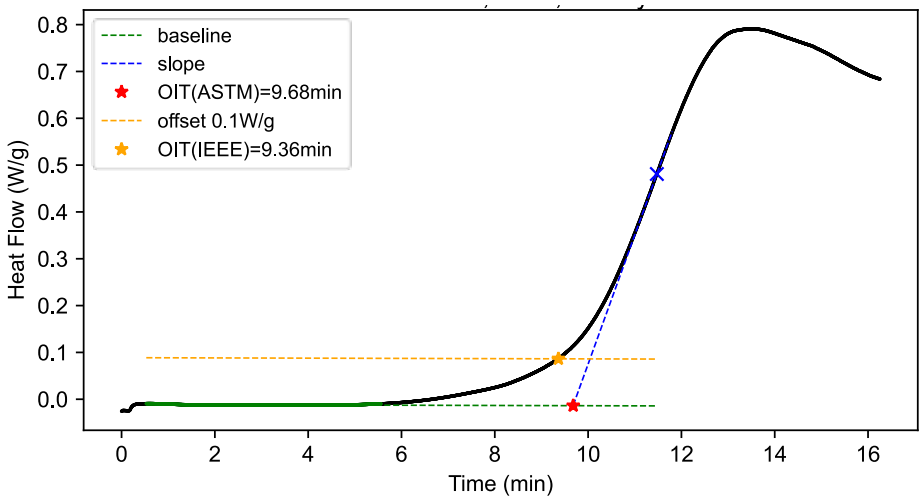

Figure 8. Determination of oxidation peak onset point as the intersection (red star) of the baseline (green dashed) and the tangent line of the exothermic peak slope (blue dashed) as described in ASTM standards, and as the intersection (yellow star) of the shifted baseline (yellow dashed) and data curve (black solid) as described in IEEE/IEC 62582-4.

OIT refers to the time elapsed since switching to O_2 as the carrier gas until the onset of the exothermic oxidation peak. The onset of oxidation peak is defined differently in ASTM standards (D3895, D4565, E1858, D3350, D5885) and in IEEE/IEC 62582-4. As illustrated in Figure 8, ASTM standards specify the onset as the intersection of the baseline and the tangent line of the oxidation peak slope, while IEEE/IEC 62582-4 obtains the onset of oxidation by shifting up the baseline by 0.1 W/g to intersect with the signal trace. Both methods were adopted when analyzing DSC data and the differences in OIT determined by the two methods were observed to be negligible (lower than 2 min for all tested samples, and lower than 0.5 min for more than 50% of the tested samples). OIT reported in section 3.2 was determined following IEEE/IEC 62582-4.

2.4.3 Yellowness Index (YI)

Yellowness index (YI) of insulation samples was measured for the initially white XLPE-D and XLPE-N samples. Artificial daylight (CIE D65) illuminant was provided by a GTI MiniMatcher MM-2e viewing system. Background lighting in the room was extinguished during image collection. A Nikon D5300 camera was mounted on a tripod and oriented towards the display panel. To optimize the quality of the collected images, the digital camera settings used were as follows: an exposure time of 1/20 s to enhance color saturation, an aperture of f/5.6 to enhance depth of field, and an ISO speed of 100 to reduce background noise. Photos were taken using a wireless remote control (Nikon ML-L3) to avoid disruption to camera orientation. Three photos were taken for each specimen. The specimen was rotated and flipped between replicate photos to minimize deviation caused by differences in light condition and camera angle at different pixel positions within a frame.

Figure 9. Photo of an XLPE-N sample next to the color reference card for calibration. Yellow boundary on the cable sample indicates the region of interest (ROI). Pixels within ROI were used for YI calculation.

Due to their specific components and internal processing, a digital camera and lens will inherently modify the color in digital images; therefore, it is necessary to map these modified colors into a system with an absolute measure of color prior to quantifying color changes in specimens tested. As shown in Figure 9, an x-rite color checker containing 24 colors was placed next to the cable sample to fit in the same photo frame. NIH ImageJ was used in conjunction with the micaToolbox to convert the collected image values to CIE XYZ color space. First, the six grey standards located on the bottom row of the color reference target were converted to reflectance values using manufacturer-supplied standard Red Green Blue (sRGB) triplets for each grey standard and then using an iterative least log slope approach to convert the triplets to reflectance values. Second, the grey reflectance values were used to create a linear normalized reflectance stack, or calibrated multispectral image, for each collected image. Third, a cone-catch model was generated based upon the charted reflectance spectra of the color reference target. Lastly, the cone-catch model was used to map the linear normalized reflectance stack to the CIE XYZ color space. Per ASTM E313, calculation of YI for a D65 illuminant is shown in Equation (1), where X, Y, and Z are the evaluated XYZ tristimulus values of the specimen.

$$YI = 100\,(1.2985 \cdot X - 1.1335 \cdot Z)/Y \tag{1}$$

2.4.4 Fourier-Transform Infrared Spectroscopy (FTIR)

FTIR is used to identify chemical changes in materials through the tracking of absorption intensities at characteristic wavenumbers. An FTIR spectrometer (Bruker Alpha II) equipped with an attenuated total reflection (ATR) attachment was used to measure the FTIR spectra of the outer surfaces of samples, at three different locations for each sample. The aged samples were pre-conditioned in a controlled environment chamber (Caron Model 7000-25) set to 23°C ± 2°C and 50% ± 10% relative humidity for at least 48 hours prior to measurment. For each spectrum, 64 scans were collected at a resolution at 4 cm^{-1} to minimize signal variation due to random noise.

2.4.5 Mass Change

An analytical balance (Mettler Toledo XPR205, 0.01 mg resolution) was used to measure the mass of the insulation specimens before and after aging.

3. RESULTS AND DISCUSSION

3.1 Elongation at Break Results

Mechanical elasticity was quantified as tensile elongation at break (EAB). As shown in Figure 10, an induction period existed where the EAB initially did not change or even slightly increased with aging time. The induction time was about 35 days at 150 °C and was about 10 days at 165 °C. After the induction period, EAB decreased with aging time and reached values below 100% absolute EAB (less than 50% of relative EAB) within the time periods explored.

The three materials did not show significant differences between their EAB performance as plotted in Figure 10. The data curves exhibit scattering around the similar trendlines. The lengths of induction times were almost the same. The time dependences (rate of decrease) of EAB in the decreasing region were also very similar. XLPE-C exhibited a slightly faster degradation rate during 10 ~ 13 days of aging at 165 °C than the other two materials. The decaBDE alternative in XLPE-N material did not affect the durability of samples aged at high temperatures, as compared to XLPE-D.

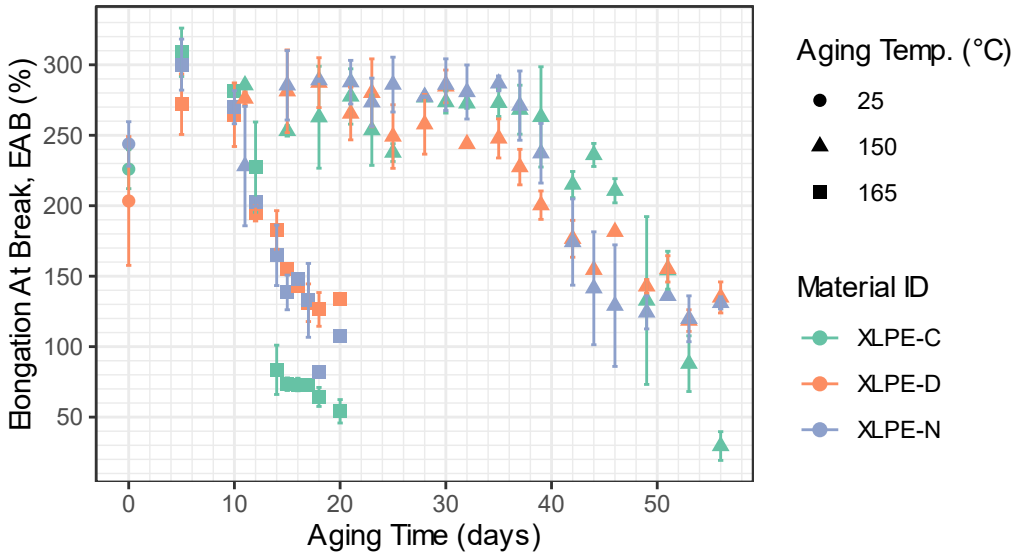

Figure 10. Tensile elongation at break (EAB) of decaBDE (XLPE-D), decaBDE alternative (XLPE-N) and commercial (XLPE-C) XLPE samples aged at 150 °C and 165 °C. Strain was determined by video extensometer.

3.2 Oxidation Induction Time Results

Oxidation induction time (OIT) is an empirical yet direct measure of the time to consume all antioxidants in the oxidative environment at a high, degradative temperature, assuming that the antioxidants will be depleted before the exothermic polymer decomposition process. Depletion of antioxidants does not cause immediate mechanical or dielectric failure of cable insulation but presages the degradation of polymer chains and subsequent embrittlement. It should also be noted that OIT is not a direct measure of flame retardancy, although certain types of flame retardants can scavenge free radicals and increase OIT.

In this study, OIT was determined for XLPE-D and XLPE-N samples exposed to pure oxygen at an isothermal temperature of 220 °C. As shown in Figure 11, OIT decreased with aging time, which is within expectation as the antioxidants are expected to be consumed in the capture of free radicals generated during thermal degradation. OIT values of shorter than 1 min were not plotted in Figure 11 as the values were too low to be reliably determined from heat flow data. Depletion of antioxidants could be noted as OIT

decreased to within 5 min, which was observed for both XLPE-D and XLPE-N materials after 6 days of aging at 165 °C and after 18 days of aging at 150 °C.

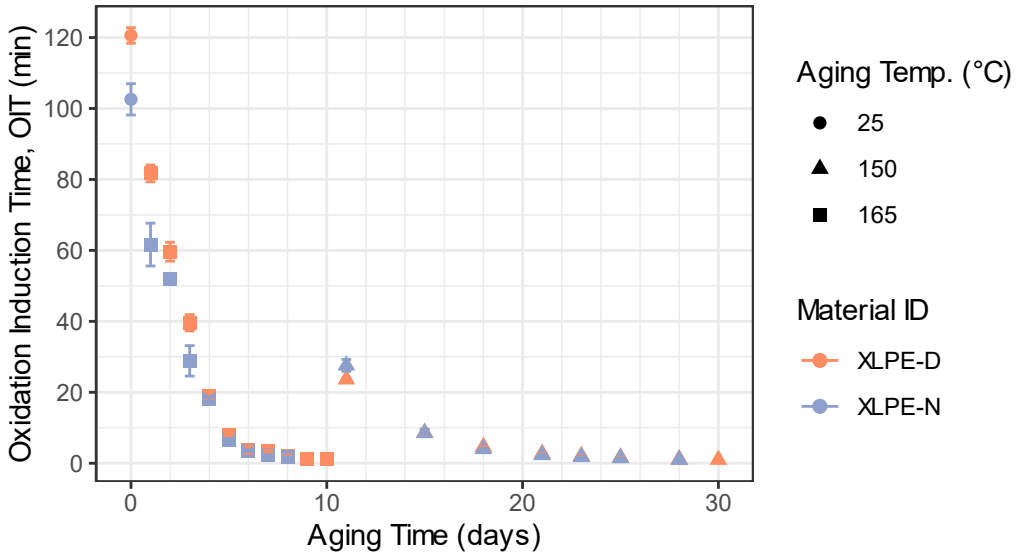

Figure 11. Oxidation induction time (OIT) of decaBDE (XLPE-D) and decaBDE alternative (XLPE-N) XLPE samples aged at 150 °C and 165 °C. The isothermal temperature for OIT test was 220 °C.

The differences between XLPE-D and XLPE-N were found in their OIT values of unaged and mildly aged samples. The unaged XLPE-D had a higher OIT (120.6 min) than the unaged XLPE-N (102.6 min). The OIT of XLPE-D samples aged for 3 days or shorter at 165 °C was also higher than that of XLPE-N. A reasonable speculation to correlate the lowering in OIT with the decaBDE alternative in XLPE-N could be that the flame retardants slightly differ and the OIT test can be considered as a controlled combustion process. As mentioned in section 1, decaBDE could release bromide radicals ($RBr \rightarrow R\cdot + Br\cdot$) to capture the reactive free radicals from polymer chains ($H\cdot$ and $OH\cdot$) which could delay the decomposition of polymers and therefore could increase OIT. However, it cannot be concluded whether the lowering in OIT in XLPE-N was due to differences in flame retardant solely, without the knowledge of the actual formulations especially the types and amounts of additives that can function as antioxidants or free radical scavengers.

3.3 Yellowness Index Results

The unaged XLPE-D and XLPE-N materials had an off-white, slightly yellow tinted, ivory color, with YI values being 50.7 and 54.5 respectively, as shown in Figure 12(a). Figure 12(b) shows increasing trends of YI with aging time for both materials. The increase was faster for XLPE-D than for XLPE-N at the very beginning of aging, i.e., within 1 day at 165 °C and within 11 days at 150 °C, after which YI of both materials showed similar aging time dependence and XLPE-D was consistently more yellow than XLPE-N. The apparent change in the speed of yellowing could be explained by the fact that more than one component in the cable insulation could cause yellowing and that different components dominate at different stages of aging.

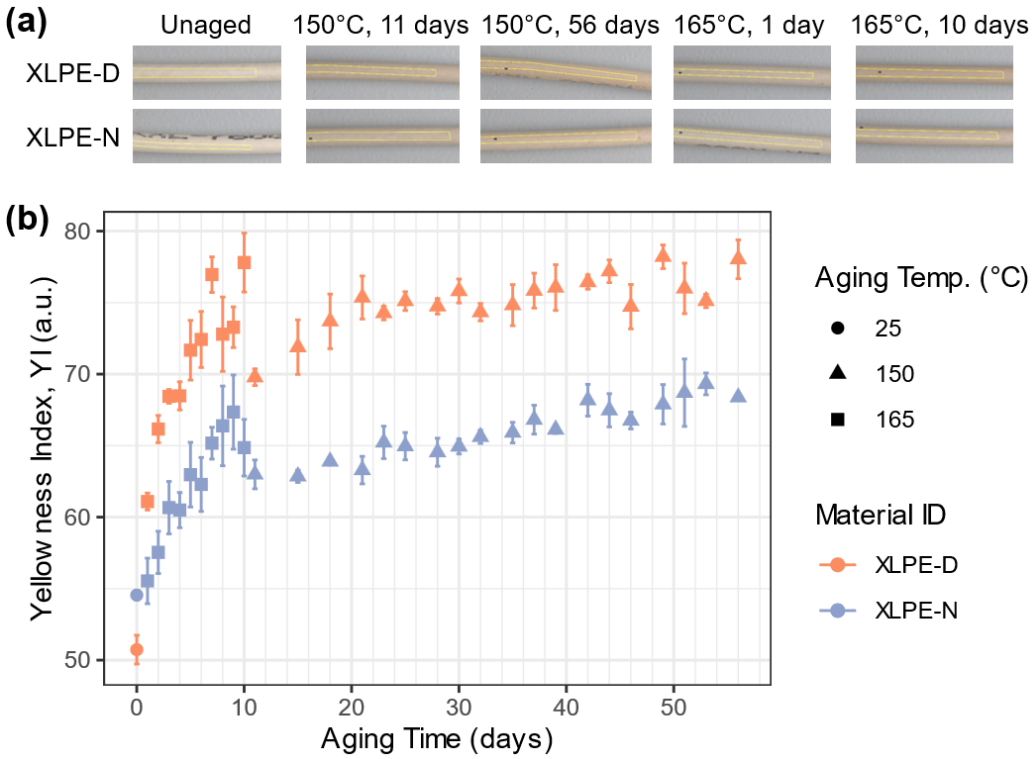

Figure 12. (a) Photos of XLPE-D and XLPE-N samples at selected aging conditions. (b) Yellowness index (YI) of decaBDE (XLPE-D) and decaBDE alternative (XLPE-N) XLPE samples aged at 150 °C and 165 °C.

Yellowing of XLPE cable insulation can be caused by yellowing of base polymer and/or additives. Polyolefins can turn yellow as a result of formation of conjugated species, such as carbonyl groups, during thermal aging. Additives such as colorants and antioxidants can also fade or turn yellow during aging. In this study, yellowing was more likely caused by discoloration of additives given that the FTIR data discussed in section 3.4 did not show oxidation peaks in the carbonyl region. Further information on chemical compositions of additives would be required to inform the exact cause of yellowing.

3.4 FTIR Results

FTIR detects changes in chemical structures of XLPE during thermal aging. The FTIR spectra for all investigated XLPE-D and XLPE-N samples are displayed in Figure 13 through Figure 16, with major peak locations labeled in the figures. The spectra showing signature peaks for generic XLPE materials are listed in Table 2.

Table 2. Absorption peak locations of XLPE.

Wavenumber (cm^{-1})	Vibrations
2916	CH_2 asymmetric C-H stretching
2848	CH_2 symmetric C-H stretching
1463	CH_2 scissoring
1350	CH_2 wagging
729, 717	Split CH_2 rocking

No peak in the region of 1700 ~ 1730 cm^{-1} for carbonyl structures of ketone and ester types was observed for aged samples. Only a shoulder was observed for XLPE-D samples aged at 150 °C for 53 days and 56 days (Figure 13). Lack of carbonyl peaks indicates that either the samples have not been sufficiently aged to cause degradation of polymer chains, or that the free radicals generated during thermal aging formed

alkenes rather than ketones or esters. Alkenes typically show absorption peaks above 3000 cm^{-1} (C-H stretching), at 1644 cm^{-1} (C=C stretching) and at 964 cm^{-1} (C-H wagging) (Smith 2016). At these three locations, a very mild and broad absorption peak above 3000 cm^{-1} could be observed for XLPE-N aged at 150 °C (Figure 14), and two small peaks near 3200 cm^{-1} and 3400 cm^{-1} were observed for both materials aged at 165 °C (Figure 15, Figure 16). The peak at 1644 cm^{-1} was apparent in Figure 15 and in Figure 16, where the peak heights increased after 1 days of aging at 165 °C for both materials and did not significantly increase at the subsequent aging periods. Lastly, the height of the peak at 964 cm^{-1} increased after aging more significantly for XLPE-N than for XLPE-D. The lack of carbonyl peaks and the increase in alkene peaks after aging indicate that the samples were aged in a relatively oxygen-deficient, i.e., pyrolytic rather than oxidative environment, which might be possible if the mobilities of radical species were high enough at the aging temperatures. Note that the FTIR measurement was performed on sample surfaces, and it is not known if oxidation was diffusion limited in these samples.

Absorption peaks showing discernable changes with aging time were those located at ~1540 cm^{-1} and ~1575 cm^{-1}, more obviously for the XLPE-N samples at intermediate aging times. Other functional groups reported to show absorption peaks in this region include metal carboxylate (COO^-), secondary amines, and aromatic –C=C stretching (Vichi 2018), (Mitra 2006). The origin of these small peaks is unknown and is suspected to be related to byproducts of crosslinking agents since these peaks existed in the spectrum of unaged XLPE-D samples.

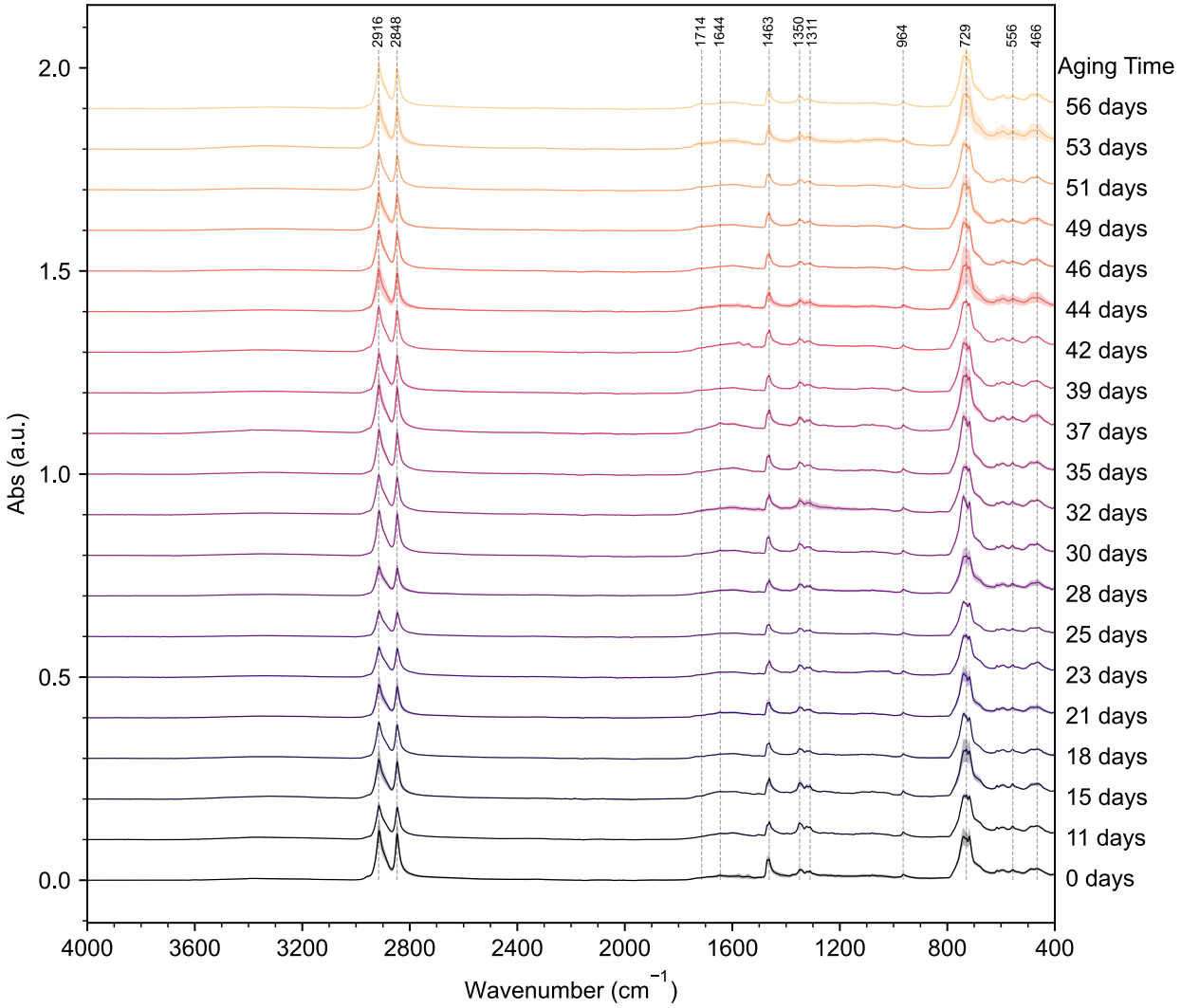

Figure 13. FTIR spectra of XLPE-D samples aged at 150 °C up to 56 days. The aging time is labeled next to the spectrum. Curves are shifted vertically for clarity. The solid lines illustrate the mean values of FTIR absorbance averaged over three replicates, and the semi-transparent band indicates standard deviations.

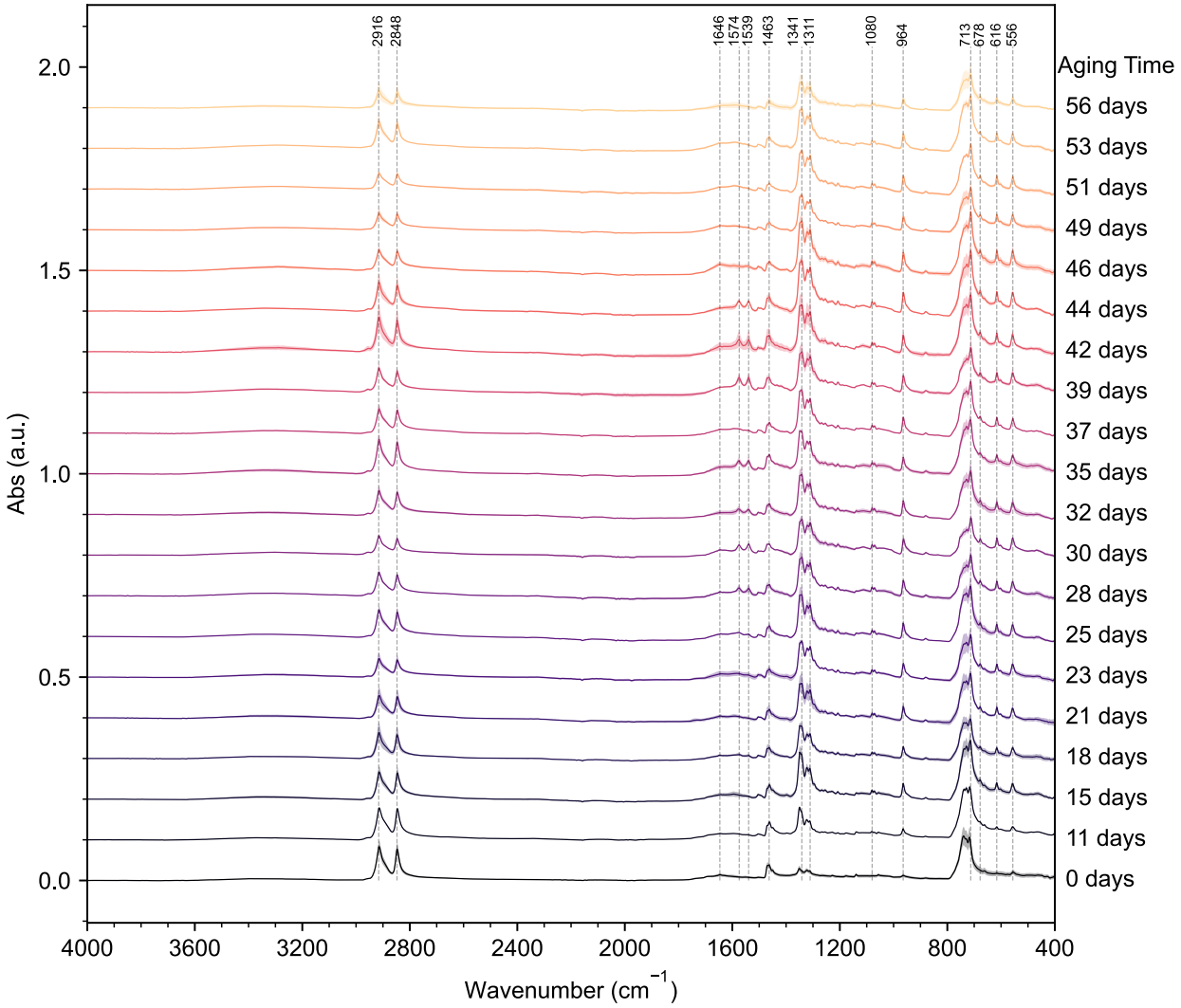

Figure 14. FTIR spectra of XLPE-N samples aged at 150 °C up to 56 days. The aging time is labeled next to the spectrum. Curves were shifted vertically for clarity. The solid lines illustrate the mean values of FTIR absorbance averaged over three replicates, and the semi-transparent bands indicate standard deviations.

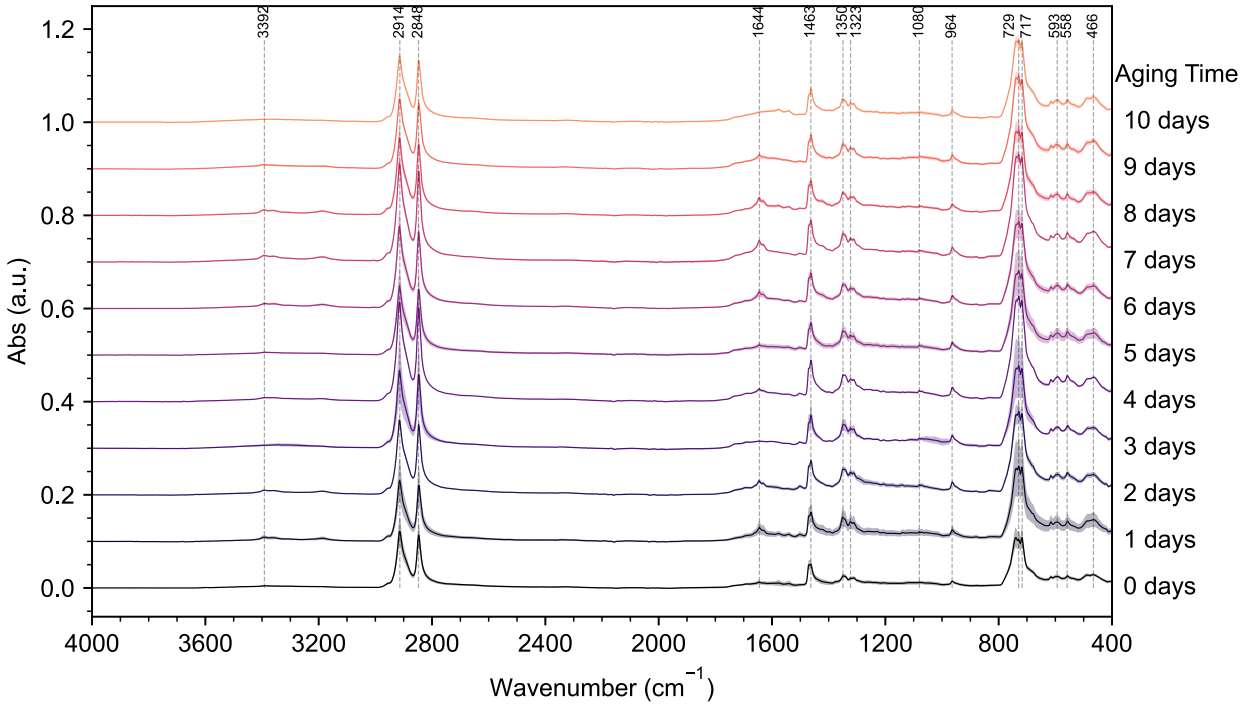

Figure 15. FTIR spectra of XLPE-D samples aged at 165 °C up to 10 days. The aging time is labeled next to the spectrum. Curves are shifted vertically for clarity. The solid lines illustrate the mean values of FTIR absorbance averaged over three replicates, and the semi-transparent bands indicates standard deviations.

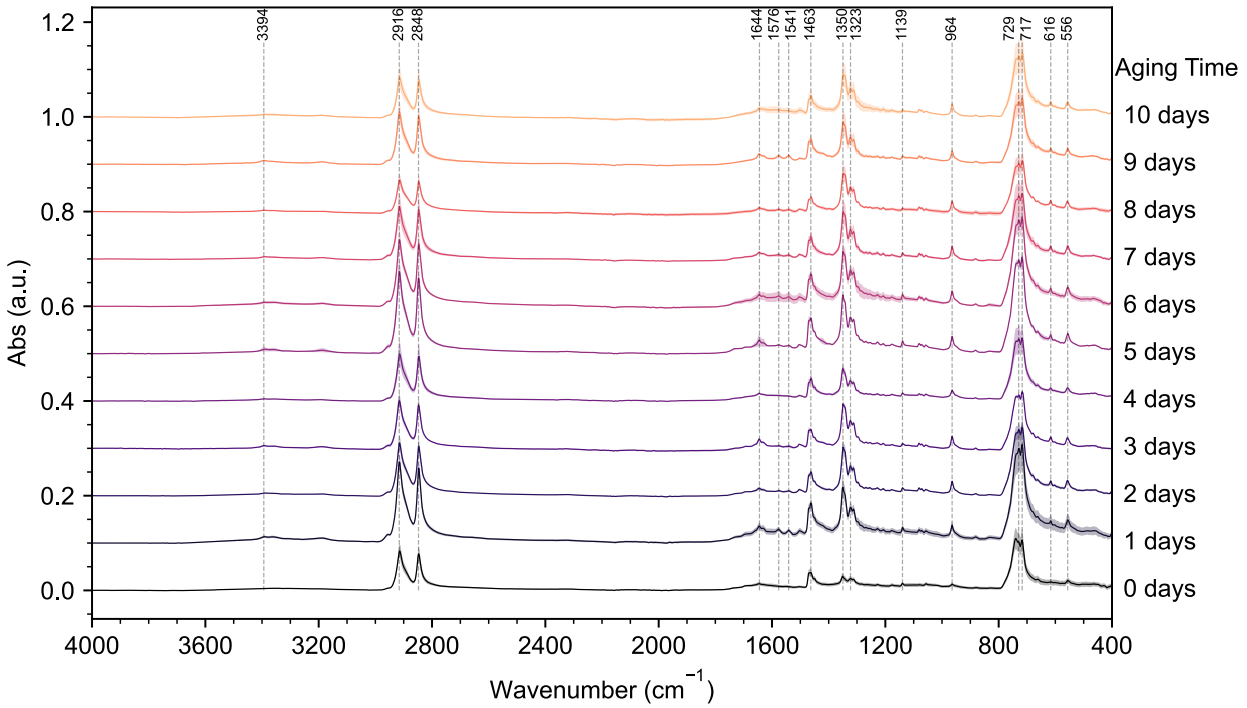

Figure 16. FTIR spectra of XLPE-N samples aged at 165 °C up to 10 days. The aging time is labeled next to the spectrum. Curves are shifted vertically for clarity. The solid lines illustrate the mean values of FTIR absorbance averaged over three replicates, and the semi-transparent bands indicate standard deviations.

Principal component analysis (PCA) was performed on FTIR data to explore the effects of variables such as material type (XLPE-D, XLPE-N, XLPE-C), aging temperature (150 °C and 165 °C), and aging time. As shown in Figure 17, data obtained for the three materials occupies different areas on the PCA biplot, which means FTIR can differentiate between the materials. Data points of XLPE-C, XLPE-D, and the 165 °C-aged XLPE-N exhibited a linear trend along the diagonal direction, while the 150 °C-aged XLPE-N dataset appeared to be more scattered and spread along the first principal component (PC1) axis, indicating that the FTIR absorption values of 150 °C-aged XLPE-N samples were less correlated between different wavenumbers than the other datasets. The contribution of variables to PC1 was plotted in Figure 18, which were uniform over the wavenumber range except for the FTIR peak locations. This indicates that the variations between materials are dependent on the overall spectrum rather than dominated by signature absorption peaks.

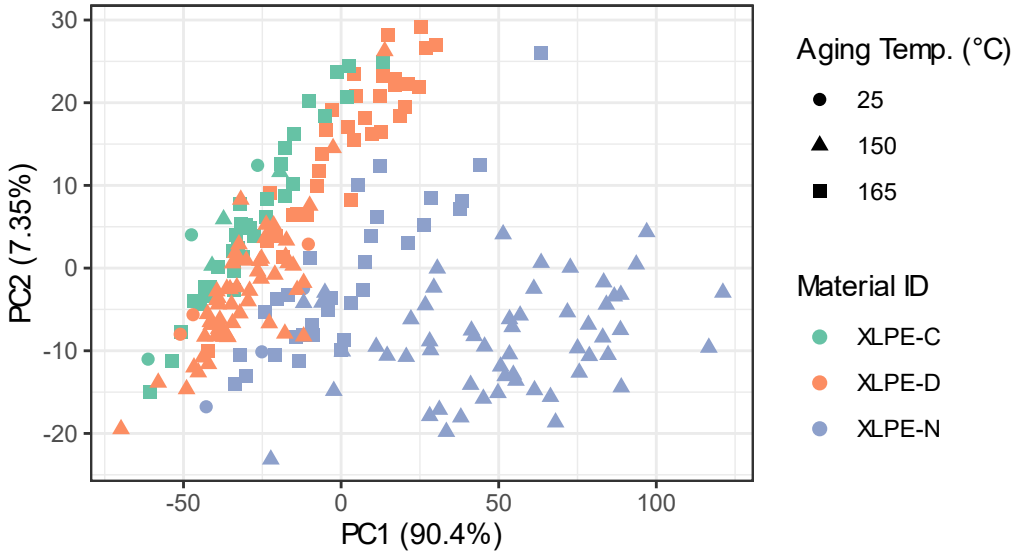

Figure 17. Principal component biplot of FTIR data of XLPE-C (green), XLPE-D (orange), and XLPE-N (purple) samples aged at 150 °C (triangle) and 165 °C (square). Unaged samples are labeled as 25 °C (circles). The principal component 1 (PC1) accounted for 90.4% of variations in the FTIR data.

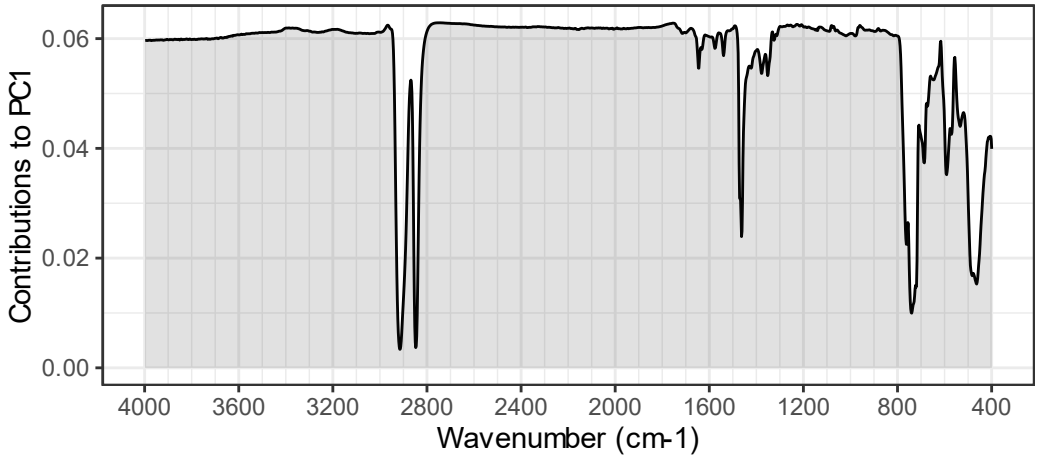

Figure 18. Contribution of variables to the first principal component (PC1), i.e., the weight of the FTIR absorbance at each wavenumber when calculating PC1 from each FTIR spectrum.

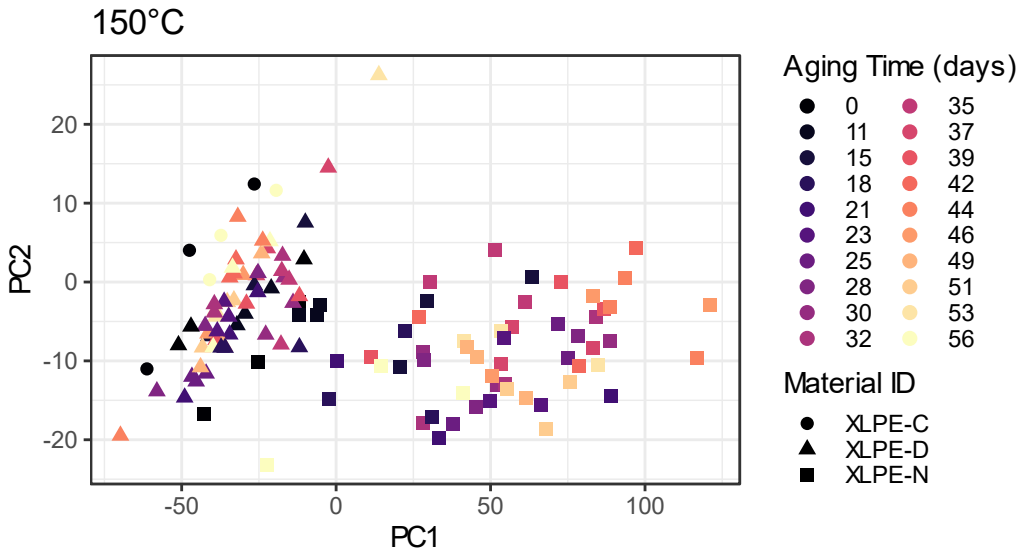

Figure 19. Principal component biplot of FTIR data of XLPE-C (circle), XLPE-D (triangle), and XLPE-N (square) samples aged at 150 °C up to 56 days (yellow, lightest). Unaged samples are labeled as 0 day (black, darkest).

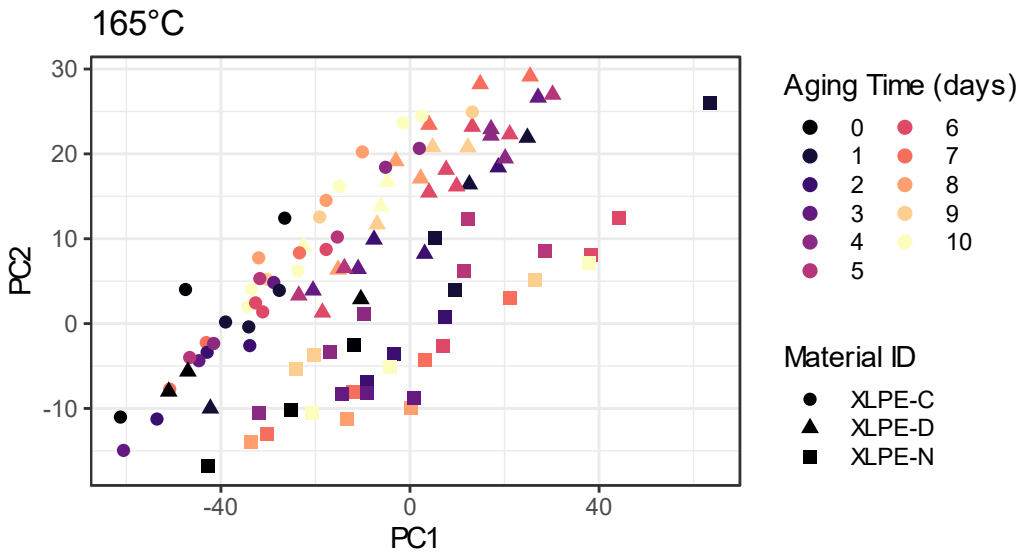

Figure 20. Principal component biplot of FTIR data of XLPE-C (circle), XLPE-D (triangle), and XLPE-N (square) samples aged at 165 °C up to 10 days (yellow, lightest). Unaged samples are labeled as 0 day (black, darkest).

Aging time did not cause systematic change in FTIR response, as can be seen in Figure 19 and Figure 20 where the data points corresponding to different aging times scatter around other data points and do not exhibit a clear trend. It is most likely that multiple reactions happened during aging and caused different changes in chemical structures of additives and the XLPE polymer, consistent with the discussions in section 3.3.

3.5 Mass Change

Mass measurement is convenient and non-destructive and sometimes linearly correlates with aging (Fifield et al. 2019). As shown in Figure 21, mass change of the aged XLPE samples showed a decreasing trend

with aging time for samples aged at 165 °C, but changed only slightly for samples aged at 150 °C. No clear differences were observed between the three materials in terms of mass change with thermal aging.

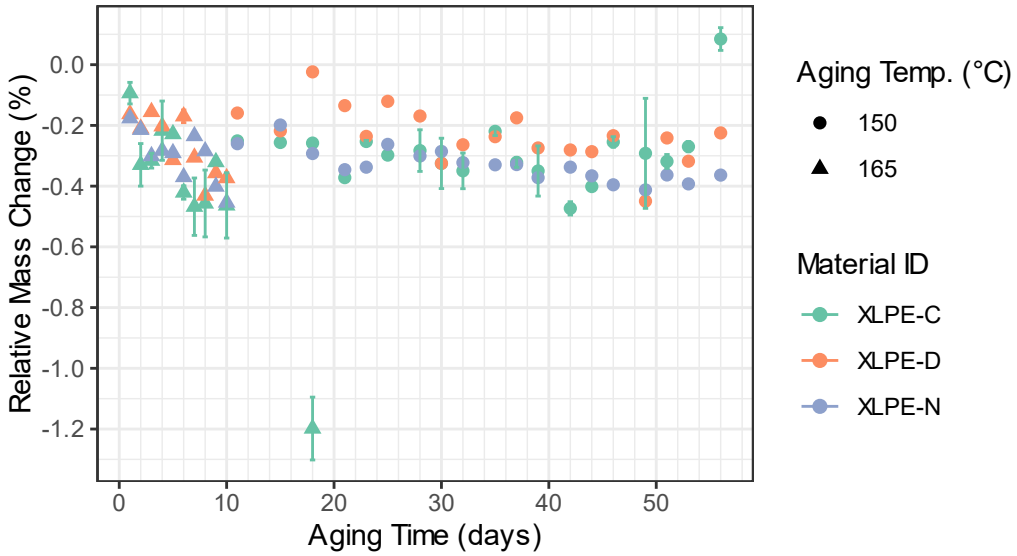

Figure 21. Relative mass change of decaBDE (XLPE-D), decaBDE alternative (XLPE-N) and commercial (XLPE-C) XLPE samples after aging at 150 °C and 165 °C.

4. CONCLUSIONS

XLPE-type cable insulation containing decaBDE (XLPE-D and XLPE-C) and XLPE with a non-decaBDE alternative (XLPE-N) were thermally aged at 150 °C up to 56 days and at 165 °C up to 20 days, and their material characteristics compared in terms of the mechanical durability (EAB), thermal stability in the oxidative environment (OIT), chemical structural changes (FTIR), discoloration (YI), and mass loss.

- Differences between XLPE-D and XLPE-N were found in their OIT values of unaged and short-term aged samples, their FTIR spectra, and their YI values. These differences may be attributed to differences in the chemical structure of the flame retardant or related differences in the composition of the insulation formulation.
- EAB was observed to decrease with aging time and reached levels below 50% of the original (unaged sample) values towards the ends of accelerated aging periods. During the induction period and the portion of the aging curve corresponding to decrease in EAB values, the studied materials XLPE-D, XLPE-N did not exhibit significant difference in their EAB performance.
- Mass of the XLPE materials was not observed to change significantly after aging in this study and cannot discriminate the differences between XLPE-D and XLPE-N.

Based on the tensile performance of XLPE-D and XLPE-N insulation samples, performance under thermal stress of the investigated RSCC XLPE insulation material does not appear to be significantly altered by the substitution of decaBDE with the selected alternative flame retardant. Further investigation including relative behavior under gamma radiation aging and combined thermal/radiation environments would also be of interest in relation to expected performance of the formulations in a design basis event such as a loss of coolant accident.

5. REFERENCES

EPRI. 2017. *Cable Polymer Material Handbook—Low Voltage Power and Control Cable*. Electric Power Research Institute 3002010637, Palo Alto, CA. https://www.epri.com/research/products/3002010637.

Federal Register. 2021. *Decabromodiphenyl Ether (DecaBDE); Regulation of Persistent, Bioaccumulative, and Toxic Chemicals Under TSCA Section 6(h),* Accessed September 3, 2024. https://www.federalregister.gov/documents/2021/01/06/2020-28686/decabromodiphenyl-ether-decabde-regulation-of-persistent-bioaccumulative-and-toxic-chemicals-under.

Fifield, L. S., M. Correa, Y. Shin, and A. J. Zwoster. 2018. *Investigation of Thermal Aging Behavior for Harvested Crosslinked Polyethylene and Ethylene-Propylene Rubber Cable Insulation.* Pacific Northwest National Laboratory PNNL-27729. Richland, WA. https://lwrs.inl.gov/Materials%20Aging%20and%20Degradation/Investigation_of_Thermal_Aging_Behavior_for_Harvested_Crosslinked_Polyethylene_and_Ethylene-Propylene_Rubber_Cable.pdf.

Fifield, L. S., Y. Ni, and M. P. Spencer. 2023. *Status of Cable Aging Knowledge Gaps Identified in the Expanded Materials Degradation Assessment (EMDA)*. Pacific Northwest National Laboratory PNNL-34863. Richland, WA. https://lwrs.inl.gov/Materials%20Aging%20and%20Degradation/EMDA_CableGaps.pdf.

Laoutid, F., L. Bonnaud, M. Alexandre, J.-M. Lopez-Cuesta, and Ph. Dubois, 2019. "New prospects in flame retardant polymer materials: From fundamentals to nanocomposites," *Materials Science and Engineering: R: Reports*, 63 (3): 100. https://doi.org/10.1016/j.mser.2008.09.002.

Mitra, S., A. Ghanbari-Siahkali, P. Kingshott, H. K. Rehmeier, H. Abildgaard, and K. Almdal. 2006. "Chemical degradation of crosslinked ethylene-propylene-diene rubber in an acidic environment. Part II. Effect of peroxide crosslinking in the presence of a coagent," *Polymer Degradation and Stability*, 91 (1): 81. https://doi.org/10.1016/j.polymdegradstab.2005.04.031.

Smith, B. 2016. "The Infrared Spectroscopy of Alkenes." *Spectroscopy.* 31 (1): 28. Accessed September 9, 2024. https://www.spectroscopyonline.com/view/infrared-spectroscopy-alkenes.

Vichi, A., G. Eliazyan, and S. G. Kazarian. 2018. "Study of the Degradation and Conservation of Historical Leather Book Covers with Macro Attenuated Total Reflection–Fourier Transform Infrared Spectroscopic Imaging," *ACS Omega*, 3 (7): 7150, https://doi.org/10.1021/acsomega.8b00773.